REPORT DOCUMENTATION PAGE

Form Approved
OMB No. 0704-0188

1. REPORT DATE (DD-MM-YYYY)	2. REPORT TYPE	3. DATES COVERED (From - To)
	Technical Papers	

4. TITLE AND SUBTITLE

Please see attached

5a. CONTRACT NUMBER
F0461-97-C-0029

5b. GRANT NUMBER

5c. PROGRAM ELEMENT NUMBER

6. AUTHOR(S)

5d. PROJECT NUMBER
4373

5e. TASK NUMBER
ODUS

5f. WORK UNIT NUMBER
346224

7. PERFORMING ORGANIZATION NAME(S) AND ADDRESS(ES)

Air Force Research Laboratory (AFMC)
AFRL/PRS
5 Pollux Drive
Edwards AFB CA 93524-7048

8. PERFORMING ORGANIZATION REPORT

9. SPONSORING / MONITORING AGENCY NAME(S) AND ADDRESS(ES)

Air Force Research Laboratory (AFMC)
AFRL/PRS
5 Pollux Drive
Edwards AFB CA 93524-7048

10. SPONSOR/MONITOR'S ACRONYM(S)

11. SPONSOR/MONITOR'S NUMBER(S)
Please see attached

12. DISTRIBUTION / AVAILABILITY STATEMENT

Approved for public release; distribution unlimited.

13. SUPPLEMENTARY NOTES

14. ABSTRACT

20030121 095

15. SUBJECT TERMS

16. SECURITY CLASSIFICATION OF:			17. LIMITATION OF ABSTRACT	18. NUMBER OF PAGES	19a. NAME OF RESPONSIBLE PERSON
					Leilani Richardson
a. REPORT	b. ABSTRACT	c. THIS PAGE	A		19b. TELEPHONE NUMBER (include area code)
Unclassified	Unclassified	Unclassified			(661) 275-5015

MEMORANDUM FOR PRR (~~Contractor~~/In-House Publication)

FROM: PROI (TI) (STINFO) 16 June 1999

SUBJECT: Authorization for Release of Technical Information, Control Number: AFRL-PR-ED-TP-FY99-0156
Krach and Sutton , "Another look at the practical and Theoretical Limits of an Expander Cycle, LOX/H_2 Engine"

AIAA JPC **(Public Release)**

ANOTHER LOOK AT THE PRACTICAL AND THEORETICAL LIMITS OF AN EXPANDER CYCLE, LOX/H_2 ENGINE

A. E. Krach*
Propulsion Sciences and Advanced Concepts Division
Air Force Research Laboratory
Wright Patterson AFB, OH 45433

A. M. Sutton†
Rocket Propulsion Engineering Division
Air Force Research Laboratory
Edwards AFB, CA 93524

ABSTRACT

Advances in materials and increases in turbopump efficiencies necessitate another look at the theoretical and practical limits for growth in chamber pressure and thrust in a liquid rocket expander cycle engine. The basic equations for turbopump power and heat flux rate out of the cooling jacket are examined to determine the theoretical limits for chamber pressure using an expander cycle. Turbopump efficiencies and operating speed limits for a LOX/H_2 expander engine are explored to determine practical limits as applied to the chamber pressure.

INTRODUCTION

The RL10 engine was the first upper stage engine to use cryogenic propellants, achieving a high specific impulse. This engine, an expander cycle, has a long history of gradual improvement. This improvement starts with the RL10A-1 engine operating at a chamber pressure of 300 psi (2,068 kPa), specific impulse of 422 seconds and 15,000 lbf (66,723 N) of thrust; and continues through the RL10B-2 operating at a chamber pressure of 640 psi (4,413 kPa), specific impulse of 466.5 seconds and a thrust level of 24,750 lbf (110,093 N)[1]. One question currently being raised for the expander cycle is how far can it grow beyond current designs in chamber pressure and thrust level? What are the limitations of the cycle?

Sutton[2] states that the expander cycle is not practical above 1,100 psi (7,584 kPa) chamber pressure since the vaporized fuel does not provide enough energy to drive the turbine to produce the higher pressures. As early as 1983[3], propulsion companies were proposing split expander engines designs operating at chamber pressures from 1,500 psi to 2,000 psi (10,342 kPa to 13,789 kPa). With new materials and improvements in turbopumps and turbopump efficiencies, another look at the practical limits of expander cycle engines is timely.

Examination of the basic equations will demonstrate the origin of the theoretical limits of the expander cycle. Understanding the theoretical limits will be useful in looking at practical limitations.

BASIC EQUATIONS

In all rockets:

$$F = Isp\, \dot{m}_p\, g \qquad (1)$$

where:

F = Thrust
Isp = Specific Impulse
$\dot{m}_p$ = Mass Flow Rate of All Propellants
g = gravitational const. g/g_c - units of (ft lbm)/(lbf s^2).

At constant Isp in any pump fed rocket, the power required to pump the propellants to the chamber increases as thrust increases, because pump power is a function of the mass flow rate of all the propellants. This pump power is also a function of turbopump pressure rise (which is much higher than chamber pressure to account for all the flow losses), and propellant density. The energy to power the pumps comes from the turbine.

* Propulsion Analyst, Member AIAA
† Project Manager, Member AIAA

Although concepts have been proposed to use all propellants for turbine drive[4] this paper will discuss split expander cycles that only use the fuel to power the turbine. For LOX/H_2 systems the hydrogen is used to power the turbines and for most engines it is a supercritical fluid within the cooling jacket and turbine. The power obtained to run the cycle is from the increased enthalpy of the hydrogen due to the energy increase from the cooling jacket.

The enthalpy of the hydrogen is increased in passing through the thrust chamber cooling channels. At constant Isp and mixture ratio, the energy requirements of the cycle increase proportionally with thrust level, which scales to throat diameter. For a fixed chamber length, the cooling jacket surface area increases with the square root of the throat area. The end result is that chamber pressure tends to decrease with larger thrust levels[5]. There are ways, however, around this surface to volume limitation and this will be addressed in the discussion of the energy equation for the cooling jacket.

The enthalpy of the hydrogen is a function of the heat flux rate of the cooling jacket. This heat transfer rate is what powers the cycle and is dependent upon the design of the cooling jacket. The governing equation is:

$$q = h_{hg} A (T_{hg} - T_{wg}) \qquad (2)$$

where:

- q = heat flux rate
- h_{hg} = hot gas side convective coefficient
- A = surface area
- T_{hg} = hot combustion gas temperature
- T_{wg} = hot gas side wall temperature .

The heat flux, $\dot{q}$, is directly related to the heat transfer coefficient, h_{hg}, surface area of the heat exchanger, A, and the temperature difference between the hot gas and thruster wall. All of these terms will be examined to determine how they affect the over all energy out of the cooling jacket.

In the chamber the heat transfer rate is fairly constant, rising sharply just before the throat and dropping rapidly in the nozzle as shown in figure 1. Any increase in heat transfer coefficient, h_{hg}, will result in a proportional increase in heat flux. Increasing wall surface roughness or lessening the fuel film biasing at chamber wall can increase the convective heat transfer coefficient, but these methods will not be addressed in this paper. Another means of increasing the convective coefficient, h_{hg}, is to increase the chamber pressure.

The heat transfer coefficient varies roughly with the gas density times the free-stream velocity to the 0.8 power[6].

$$h_{hg} \sim (\rho V)^{0.8} \qquad (3)$$

where:

ρ = density of propellant
V = velocity of hot gas .

Since density and velocity are proportional to chamber pressure, increasing the chamber pressure will increase the heat transfer coefficient by the 0.8 power of the chamber pressure. The effects of this increase with respect to the chamber pressure will be discussed later.

The effect of surface area on the heat flux is straightforward. Any increase in the surface area or heat transfer coefficient will result in a proportional increase in the heat flux. Adding heat exchanger surface area in the nozzle is less effective than adding surface area in the combustion chamber and throat regions as can be seen in figure 1. Increasing the surface area for the combustion chamber and cooling jacket is a primary method for increasing the heat transfer rate and dealing with the surface to volume limitations for the higher thrust levels[7]. Many methods have been proposed for increasing surface area. These include heat exchanger inserts within the combustion chamber, ribbed chamber walls, fins within the chamber and plug nozzles.

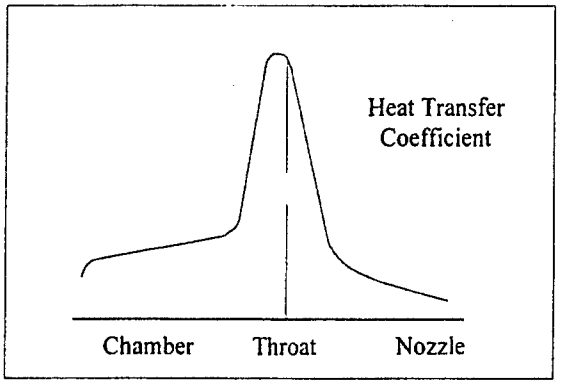

Figure 1. Heat transfer coefficient vs. chamber length.

A practical limitation of increasing chamber length is the weight penalty associated with an increase in surface area. A trade between engine weight and increasing surface area is difficult because it is dependent upon a specific design where engine volume, the needed Isp and nozzle area ratio are set by system designers; each specific chamber design will have limits set by material properties, and manufacturing processes. Since initial trades do not generally have that level of detail, weight estimates then depend on scaling algorithms based upon existing engines. These estimates are generally acceptable for examining trends but are less than satisfactory in determining specific

design weights. This is especially true if the design being traded is far from the design points upon which the weight estimation algorithm is based.

The wall temperature and chamber gas temperature will also influence the heat flux. However, the variation in the temperature difference that can be practically achieved is not as great as can be gotten by changing the heat transfer coefficient or adding surface area to the heat exchanger. This is evident by examining both hot gas and chamber sidewall temperatures. The hot gas temperature is a function of propellant mix ratio and chamber pressure. An increase of about 1,000 psi (6,895 kPa) in chamber pressure will result in an increase in hot gas temperature of less than 5%. Optimum engine operation requires a narrow range for mix ratio. For optimum operation, changes in mix ratio will be small and therefore will not significantly affect the chamber temperature. The hot gas wall temperatures also can be changed by increasing the number of cooling circuits or passages, by increasing the thermal conductivity of the chamber material, altering channel geometry or other means. However, even significant changes in hot gas wall temperature will not significantly affect the temperature difference and therefore overall heat transfer rate. The following example illustrates this.

If the gas temperature is 6,000°F (3,316°C) and the hot gas wall temperature is 1,000°F (538°C), the temperature difference is 5,000°F (2,760°C). If the thermal conductivity of the material is higher or the cold side convective coefficient increases, then the hot gas wall temperature will drop. If the hot gas wall temperature goes from 1000°F to 100°F (38°C) the temperature difference becomes 5,900°F (3,260°C), an improvement of 18% for a hot side wall temperature decrease of 900°F (482°C). A temperature curve for a counter flow heat exchanger is shown in figure 2. The dashed line notionally shows the gains that may be obtained in temperature difference through modifying the design of the cooling jacket.

For a single pass counter flow heat exchanger the temperature difference will tend to remain constant with increasing surface area. There will be a temperature limit approached for the coolant out. This temperature limit is probably not a practical one since the surface area needed to approach this limit would be too great when the weight is considered.

A practical wall temperature lower limit is at the point where condensation forms on the inner wall of the chamber due to the cooling of the hot gas wall. Additionally, a practical wall temperature upper limit exists at the point when the wall material either losses strength due to hot temperature or thermal cycling. As previously shown, the primary methods for increasing the heat flux is by increasing the surface area and the convective heat transfer coefficient.

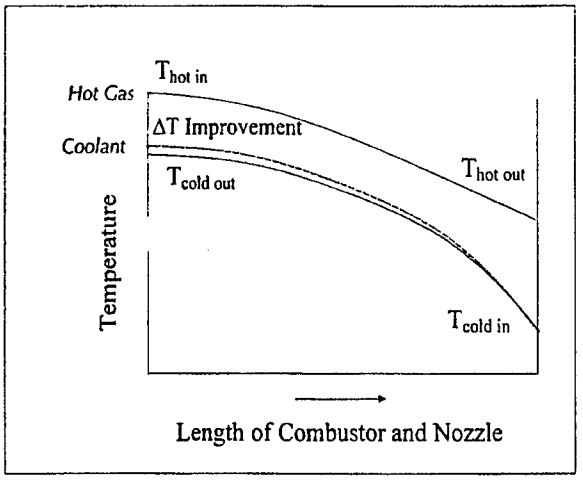

Figure 2. Temperature distribution for a single pass counterflow heat exchanger.

The heat that is picked up in the combustion chamber and nozzle cooling jackets is what powers the turbine in the cycle. The equation for power out of the turbine is:

$$P_t = \eta\, m_f\, g\, \Delta H \qquad (4)$$

where:

η = efficiency

m_f = fuel mass flow rate

g = gravitational const. g/g_c - units of (ft lbm)/(lbf s^2)

ΔH = change in enthalpy.

As indicated earlier the power requirements of the pumps increase proportionally with thrust level. The power created by the turbine, in an expander cycle, is dependent upon the mass flow rate of the fuel and the increase in enthalpy provided by the cooling jackets. However, as can be seen from the full and split expander cycles in figures 3 and 4, not all the hydrogen fuel is needed to power the turbines.[8] For a given thrust, since the mass flow can be increased into the turbine for a split expander cycle, the heat that can be obtained from the jacket is not limited by the temperature of the coolant out of the jacket.

As thrust increases, at constant Isp and mixture ratio, the mass flow rate of the fuel also increases providing more power to the cycle. The power consumed by the pumps also increases with the increase in mass flow and thrust.

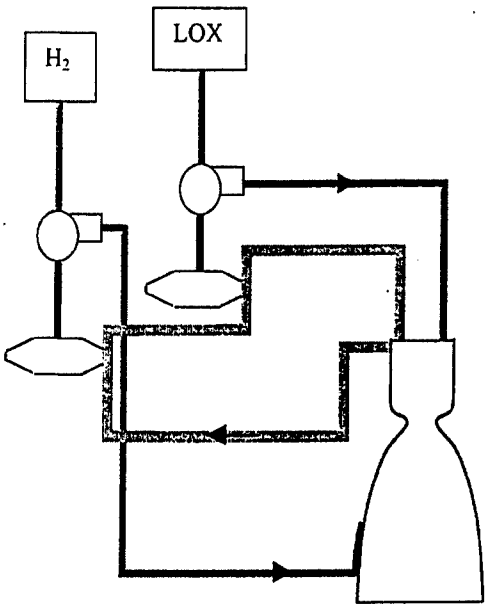

Figure 3. Expander Cycle

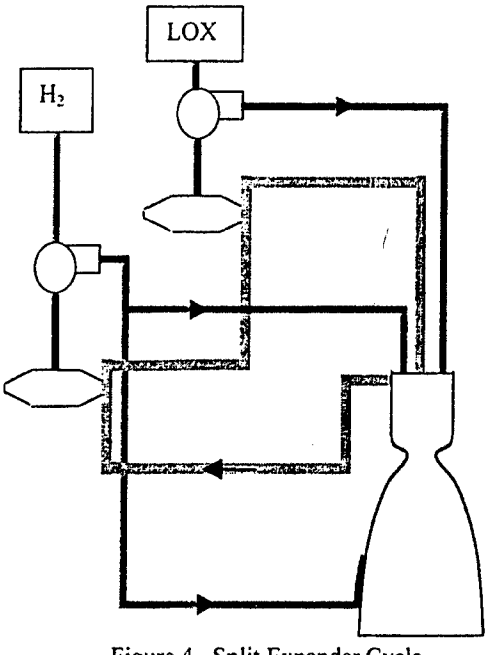

Figure 4. Split Expander Cycle

For an increase in the heat transfer rate of the cooling jacket, due to either an increase in surface area or an increase in the convective heat transfer coefficient, what increase can be expected from the pump discharge pressure? If the chamber pressure in the engine is increased, what increase will be seen in the convective heat transfer coefficient and ultimately in the pump discharge pressure due to the increase in the heat transfer rate out of the cooling jacket?

For a given pump, the flow rate, head and power are all related to the speed, N, of the pump. For a centrifugal pump, it is directly proportional to the turbine shaft speed. For a pump the relationships are given as:

$$\Delta P \text{ (pressure change across pump)} \sim N^2$$

$$P_p \text{ (pump power)} \sim N^3$$

This gives the relationship for the increase in pressure for the pump for an increase in the heat transfer rate Q out of the cooling jacket if the mass flow rate stays the same. This can be simply given as the Q factor to the 0.66 power. In figure 5, these factors are shown plotted with one another. A 500 psi (3,446 kPa) chamber pressure engine was used as the base. The chamber pressure is varied from 500 psi to 2,500 psi (17,228 kPa). Chamber pressure was normalized by the base chamber pressure 500 psi, so the chamber pressure factor ranges from 1 to 5. The cooling jacket surface area in determining these factors is assumed to grow proportionately to the chamber pressure. This is counter to what is seen in a staged combustion or gas generator since for those cycles an increase in chamber pressure results in a smaller thruster. This is not the same for an expander engine, which needs to maintain surface area in order to power the cycle. As previously shown, the heat transfer rate changes with the ratio of the chamber pressures to the 0.8 power.

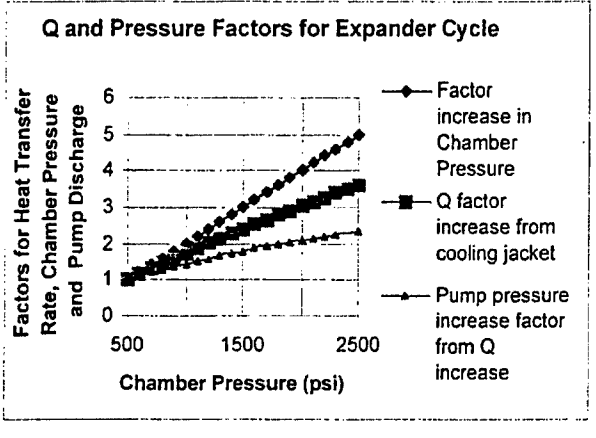

Figure 5. Heat and Pressure Factors for Expander Cycle Engine.

Figure 5 shows the increase in pump discharge pressure due to an increase in Q. The actual increase in chamber pressure due to an increase in the heat transfer rate out of the jacket is also influenced by system pressure losses. While pressure drop across the injector represents a significant portion of the system losses and should increase with chamber pressure, the pressure

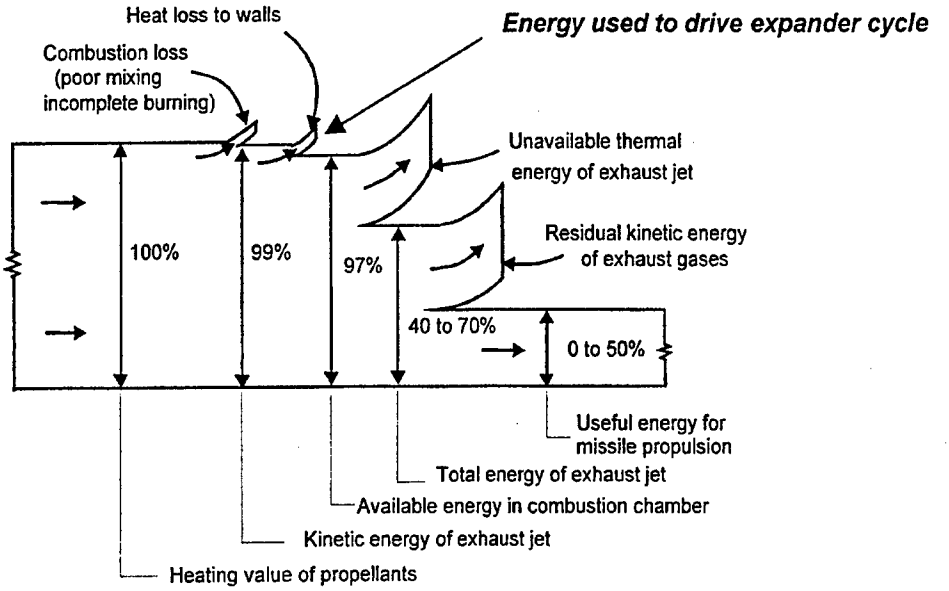

Figure 6. Energy balance diagram for chemical rocket

in the cooling jacket can also be significant and will increase with the increase in enthalpy of the coolant. As the density of the hydrogen decreases, the fluid is more difficult to pump. This effect is shown later in the results from the engine balance in figure 9, but an example will be illustrative. Taking a turbine efficiency of 0.8, a pump efficiency of 0.7 and varying system efficiency from 0.7 to 0.9 gives an overall gain in chamber pressure of 0.4 to 0.5 for an addition of heat to the jacket.

Sutton[9] shows in figure 6 that the energy available within the chamber for propulsion is actually only a portion of total energy in the propellant with a significant proportion lost. The total heat flux rate out of the cooling jacket is largely influenced by available surface area. Power to run higher chamber pressures and thrust levels than current designs should be available given enough surface area for the cooling jacket. Further if a higher chamber pressure is attainable, then the convective heat transfer coefficient is also increased.

CONSIDERATIONS FROM ENERGY BALANCE

Energy balances were performed on full and split expander cycle engines. The difference between the two is in the fuel mass flow through the turbine and cooling jacket. The split expander has a penalty of reduced mass flow through the turbine, however this reduced flow also decreases pressure loss through the cooling jacket, which translates to reduced pump power. In the energy balances that were performed the split expander was able to achieve a higher performance and chamber pressure, based on assumed turbine efficiencies and cooling pressure loss.

The energy balances on the split expander cycle engines thrust ranged from 50,000 and 65,000 lbf (222,400 and 286,000 N), with chamber pressures ranging from 1,375 to 2,300 psi (9,480 to 15,858 kPa). In examining the energy to balance the required pump power relative to various chamber pressures, the plotted curve is fairly linear as shown in figure 7. It should be noted that the first data point for a chamber pressure of 475 psi (3275 kPa) was for the RL10A-3-3A engine. The remaining data points were for a split expander cycle. Since the RL10 is a full expander engine and not a split expander cycle, the two cycles are not directly comparable. The data for the RL10 engine is included in order to see where a current engine would be plotted.

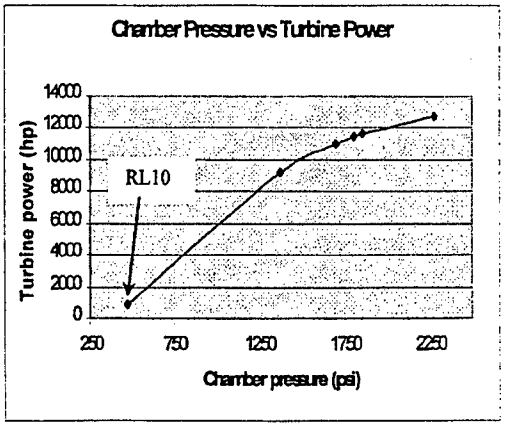

Figure 7. Chamber Pressure vs. Turbine Power

Thrust was kept constant, chamber pressure was optimized and Isp allowed to vary. Engine balance calculations were performed for steady state conditions with the turbine and pump efficiencies somewhat higher than for current operating engines. These efficiencies for the turbopumps should not warrant extensive development, however, and should be possible under the current state of the art. The hydrogen pump isentropic efficiency ranged from 60% to 67%. The oxygen pump efficiency was set to 75%. Fuel turbine efficiency was assumed to be from 82 to 83% and oxygen turbine isentropic efficiency was assumed to be 85%. The engine balances indicate that for chamber pressures ranging from 1,375 psi to 2,300 psi (9,480 to 15,858 kPa), the power required for the turbine grows at a linear rate. The operating speed of the hydrogen turbopumps is extremely high compared to existing engines. Turbopump shaft speeds for the varying chamber pressures ranged between 115,000 and 193,000 rpm.

Shaft speed has typically been limited first by conventional roller element bearing speed limits and then by turbine stresses. The product of the shaft diameter and shaft speed, DN, expresses the rotordynamic limit in units of in/ RPM (mm/RPM).

Historically roller element bearings in liquid hydrogen have been limited to 78,740 in/RPM (2,000,000 mm/RPM). This translates to LH_2 turbopump speeds of 25,000-50,000 RPM for this thrust class engine[10]. The DN limits can be overcome by the use of hydrostatic bearings. The Air Force is building an Advanced Liquid Hydrogen Turbopump, for a 50,000 lbf (222,400 N) thrust, that has a rotational speed of 175,000 RPM using hydrostatic bearings[11].

This shaft speed is in excess of the current AN^2 limits for state of the art materials. AN^2 is defined as the product of turbine annulus area and the square of shaft speed. This will not affect the ability to operate at the higher chamber pressures. If the shaft speed must be reduced to meet current material AN^2 limitations, the result will be a slower, heavier turbine. The chamber pressure will remain the same. This means that weight as well as turbine life issues become the factors that are traded against chamber pressure. Again, weight estimation is difficult because of being design specific. Other studies show that higher chamber pressures with $LO2/H_2$ propellants are attainable with similar operating conditions[12].

For a given thrust and Isp, throat area will decrease as chamber pressure increases. Several balances were run increasing the heat transfer rate in the jacket from 25,000 Btu/sec to 30,000 Btu/sec, (26,375 kW- 31,650 kW) maintaining a constant thrust and Isp within 1 sec of 461 seconds. Figure 8 shows how the heat exchanger surface area changes with an increase in chamber pressure.

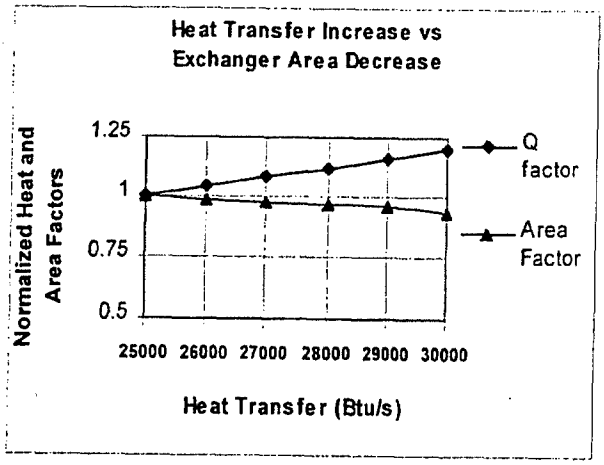

Figure 8. Heat Transfer Rate Increase vs. Heat Exchanger Area Decrease

The factor for heat transfer, Q, is arrived at by normalizing the heat transfer rate with the baseline case of 25,000 Btu/sec. The surface area factor is simply the square root of the throat area divided by the baseline throat area, assuming that the length of the cooling jacket is constant. However, this is not realistic since surface area must increase to accommodate the increase in chamber pressure. So while the throat area is getting smaller the cooling jacket surface area must increase by some means to provide the additional heat transfer surface for the added Q. This normally means an increase in the pressure drop across the jacket due to the increase in surface area.

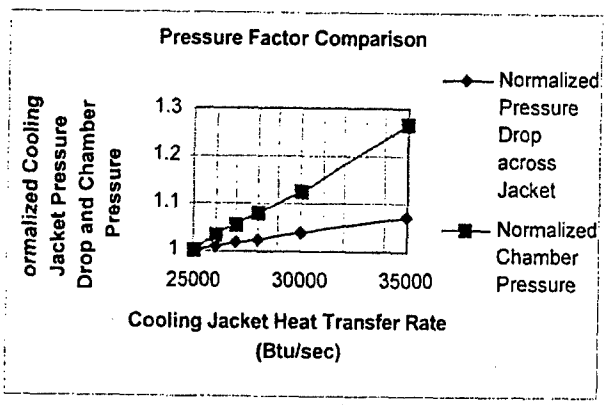

Figure 9. Comparison of Normalized Chamber Pressure and Normalized Pressure Drop across Cooling Jacket

In order to quantify the effect of increasing pressure drop across the cooling jacket for increasing heat transfer rate in the cooling jacket, additional engine balances were made. For a full expander cycle, a given thrust and Isp, several cases were run, increasing the heat transfer rate in the jacket from 25,000 Btu/sec to 35,000 Btu/sec (26,376 to 36,927 kW). The results are shown in figure 9. The pressure drop across the jacket was normalized by the pressure drop across the cooling jacket for the case where the heat transfer rate out of the cooling jacket of 25,000 Btu/sec. The chamber pressure was normalized by the chamber pressure for the case where the heat transfer rate out of the cooling jacket of 25,000 Btu/sec.

Pressure drop increases for split expander cycle engines in the cooling jacket due to an increase in the heat transfer rate may be less due to less total flow in the jacket than for a full expander cycle.

CONSIDERATIONS FROM HEAT TRANSFER ANALYSIS

A heat transfer analysis was run for the above cases using the Two Dimensional Kinetics (TDK) boundary layer module (BLM) to calculate an approximate heat flux rate out of the jacket. By stretching the chamber length and thereby increasing the surface area of the cooling jacket the heat transfer rates necessary for the turbines and corresponding chamber pressures were met. The heat transfer rate was able to grow linearly with respect to chamber pressure as seen in figure 10.

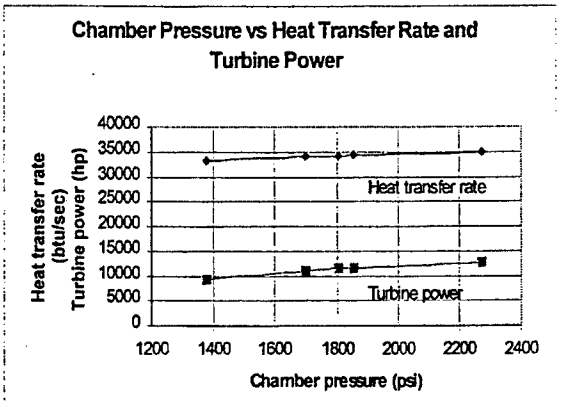

Figure 10. Chamber Pressure vs. Heat Transfer Rate and Turbine Power

The heat flux rate calculated by TDK was verified by a finite element analysis modeling a single tube for an 1,800 psi (12,411 kPa) chamber pressure, 65,000 lbf (289,000 N) thrust engine

CONCLUSIONS

The analysis of the expander cycle designs shows that at steady state, the heat flux out of the chamber and nozzle cooling jacket provides enough energy to run the turbopumps to obtain higher chamber pressures. This analysis shows that chamber pressure range of 1,375 psi to 2,300 psi (9,480 kPa to 15,858 kPa) is possible in the expander cycle engine for thrust levels of 65,000 lbf (289,000 N).

The analysis addresses the three primary factors that drive the cycle. The heat transfer analysis shows that the amount of heat out of the jacket seems to be reasonable. Turbopump operating speed limits have significantly increased, pushing up the practical limits for the chamber pressure via the use of hydrostatic bearings. Hydrostatic bearings greatly reduce bearing caused speed limitations. Since the geometry of the nozzle can be varied to increase the amount of heat gained from the chamber and nozzle cooling jackets higher chamber pressures are obtainable.

The practical limits for the expander cycle are driven by materials properties such as those associated with strength at high temperatures and compatibility with propellants. Since the energy balance for the different chamber pressures dealt only with steady state conditions further considerations addressing start-up and transient states are recommended. The transient studies would gain in importance at the higher thrust levels.

It is difficult to set an absolute theoretical limit on maximum chamber pressure obtainable for the cycle due the ability to increase surface area and thus increasing heat transfer rate out of the cooling jacket. Increasing surface area of the combustion chamber will increase in the heat transfer rate out of the cooling jacket providing the necessary energy for the turbine. Determining the practical limits of surface area increases is difficult due to system design, material properties, and manufacturing processes. This also holds true for the determination of the turbine size due to the limitation on shaft speed. Ultimately, since greater surface area for the cooling jacket and a higher convective heat transfer coefficient can increase the heat transfer rate to power the cycle, the practical limit for the expander cycle itself for the higher chamber pressures as well as thrust levels becomes a weight trade.

ACKNOWLEDGEMENTS

The authors are grateful to George P. Sutton for the time he spent reviewing this paper. His comments are greatly appreciated.

REFERENCES

[1] Santiago, Jorge R., "Evolution of the RL10 Liquid Rocket Engine for a New Upper Stage Application," 32nd AIAA/ASME/SAE/ASEE Joint Propulsion Conference, 1996, AIAA 96-3013.

[2] Sutton, George P., *Rocket Propulsion Elements*, 5th edition, Wiley & Sons, New York, 1986, pg. 156.

[3] Cooper, L. P., "Advanced Propulsion Concepts for Orbital Transfer Vehicles," AIAA/SAE/ASME 19th Joint Propulsion Conference, 1983, AIAA-83-1243.

[4] Buckmann, P. S., et. al., "Design and Test of an Oxygen Turbopump for A Dual Expander Cycle Rocket Engine," 25th AIAA/ASME/SAE/ASEE Joint Propulsion Conference, July 1989, AIAA 89-2305.

[5] Crocker, A. & Peery, S., "System Sensitivity Studies of a LOX/Methane Expander Cycle Upper Stage Engine," 34th AIAA/ASME/SAE/ASEE Joint Propulsion Conference, July 1998, AIAA 98-3674.

[6] Huzel, D. K., Huang, D. H., *Modern Engineering for Design of Liquid-Propellant Rocket Engines*, Volume 147, Progress in Astronautics and Aeronautics, AIAA, Washington DC, 1992, pg. 85.

[7] Tanatsugu, N. & Suzuki, K., "The Study of High Pressure Expander Cycle Engines with Advanced Concept Combustion Chamber," 35th Congress of the IAF, Lausanne, Switzerland, October 8-13, 1984, Acta Astronautica, Vol. 13 No. 1. pp. 1-7. 1986.

[8] Masters, A. I. & Tabata W. K., "Advanced Expander Test Bed Engine," AIAA/NASA/OAI Conference on Advanced SEI Technologies, Sept 1991 / Cleveland. OH, AIAA 91-3437.

[9] Sutton, op. cit., pg. 28.

[10] Henderson, T. W. & Scharrer, J. K., "Hydrostatic Bearing Selection for the STME Hydrogen Turbopump," 28th AIAA/ASME/SAE/ASEE Joint Propulsion Conference, 1992, AIAA 92-3283.

[11] Minick, A. & Peery, S., "Design and Development of an Advanced Liquid Hydrogen Turbopump," 34th AIAA/ASME/SAE/ASEE Joint Propulsion Conference, July 13-15, 1998 / Cleveland, OH, AIAA 98-3681.

[12] Martinez, A. & Fulton, D. L., "Advanced LOX/H_2 Engines Technologies for Future OTVs," 19th AIAA/ASME/SAE/ASEE Joint Propulsion Conference, Jun 1983 / Seattle, WA. AIAA 83-1312.